

Preparation and characterization of coated nanoscale Cu/SiC_p composite particles

Rui Zhang^{a,b}, Lian Gao^{a,*}, Jingkun Guo^a

^aState Key Lab of High Performance Ceramics and Superfine Microstructure, Shanghai Institute of Ceramics, Chinese Academy of Sciences, Shanghai 200050, China

^bCollege of Materials Engineering, Zhengzhou University, Henan 450003, China

Received 18 April 2003; received in revised form 29 April 2003; accepted 2 June 2003

Abstract

Nanoscale Cu/SiC_p composite particles were prepared using a coating method. XRD, AES, SEM, DSC-TG-MS techniques were used to characterize the coated composite particles. It was found that a core-shell structure is constructed in the coated Cu/SiC composite particles with the core of SiC and the shell of Cu. A new layer of Cu₂O is created on the surface of the coated particles due to the oxidation of nano Cu crystallites. The expected sintering temperature for the coated Cu/SiC composite particles is below 950 °C.

© 2003 Elsevier Ltd and Techna S.r.l. All rights reserved.

Keywords: A. Sintering; B. Nanocomposites; D. SiC

1. Introduction

In recent years, Cu/SiC composites have received considerable attention to meet the challenges of thermal management in the rapidly increased power of advanced electronics. They offered a great potential for uses in high-temperature structural applications and electronic packing due to the superior heat-conductive, electric-conductive and heat-releasing natures [1–3]. The poor compatibility between SiC and Cu was the most concern in the preparation of Cu/SiC composites [4,5]. Many efforts have been focused on the development of compatibility-enhancing procedures. Coating technology (instead of an admixture method) was one of the appreciable ways [6–9]. Nevertheless, most of the as-reported copper/SiC composites were prepared by coating copper on SiC whiskers or particulates in dimensions of microns. No open literature about coating copper on nano SiC particles had been reported thus far. Strategically, nano copper/SiC_p composite particles might be more attractive, since unique electrical, thermal,

mechanical properties had been found in nano-structured composites [10,11].

In this study, an electroless coating method is used to prepare nano Cu coated SiC particles. The surface condition and sintering behavior of the coated composite particles are investigated.

2. Experimental

SiC particles (~120 nm in average diameter; China Huatai Group) were commercially available. Cu was obtained by displacing Cu²⁺ ion with Zn powder during a cementation reaction. The ratio of Cu to SiC is 75:25 (vol.%). During the coating process, the aqueous suspension at pH 2 containing the SiC particles was ultrasonicated for 30 min and blended into a saturated CuSO₄ solution in a round-bottomed flask. The flask was mounted onto a rotating apparatus at a 45° angle. Two-thirds of the flask was immersed in a 30 °C water bath. Very fine particles (or crystallites) in the solution precipitated as the flask rotated centrifugally. After 10 min, the high-purity Zn powder was added to the flask. The relative amount of Cu/SiC to Zn powder was 53:47 (wt.%). The rotation rate was ~240 rpm (round per minute). After 30 min, the final deposition of particles

* Corresponding author. Tel.: +86-21-52412718; fax: +86-21-52413122.

E-mail address: liangaoc@online.sh.cn (L. Gao).

was filtered, rinsed, and dried at 80 °C. The morphology of particles was observed using a field-emission scanning electron microscope (SEM; Jeol JSM-6700F). Surface elements of coated particles were detected by Auger electron spectra (AES; Microlab 310-F). Phases in the coated composite powders were identified by X-ray (CuK_α) diffraction analysis (XRD; D/MAX - 2550V, Rigaku Tokyo, Japan). The surface composition of

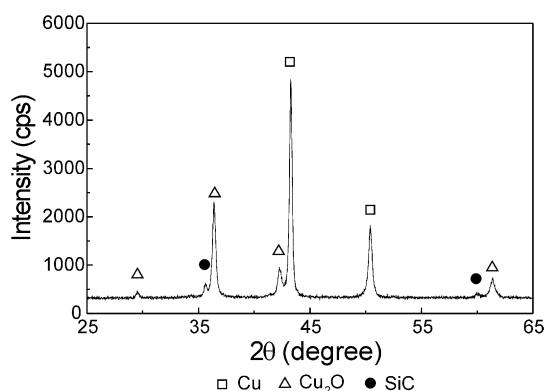


Fig. 1. The XRD pattern of the coated composite particles.

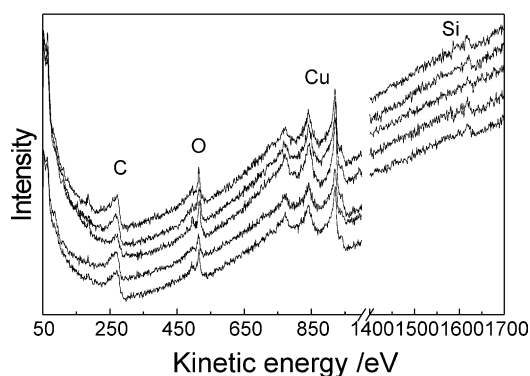


Fig. 2. The AES patterns of the coated composite particles corresponding to 5 different areas ($1 \times 1.2 \mu\text{m}$).

different samples was confirmed through the zeta potential measurement (Zetaplus, Brookhaven, NY). The average particle size was estimated according to Scherrer formula:

$$D = 0.89\lambda / (\beta \cos \theta) \quad (1)$$

where D is the average diameter of the grains, λ the wavelength of X-ray, $\beta = (B - 0.15)$ the full width at half maximum of the diffraction line (111), θ the Bragg angle. The sintering behavior of the coated Cu/SiC_p composite particles was determined using the differential scanning calorimetry (DSC) and thermogravimetry (TG) (STA 449C, Netzsch, Germany), coupled with quadrupole mass spectrometer (MS) (QMG-511, Balzers, Switzerland) (DSC-TG-MS). The heating was conducted in flowing Ar gas (20 ml/min flow) with the heating rate of 10 °C/min. Al_2O_3 crucible was employed as the reference material.

3. Results and discussion

Fig. 1 shows the XRD pattern of the coated composite particles, indicative of the presence of Cu, Cu_2O and SiC. The inherent Cu_2O is formed due to the instantaneous oxidation of Cu during the coating process [12]. The AES patterns of different areas in dimension of $\sim 1 \times 1.2 \mu\text{m}$ are given in Fig. 2. Note that Si, C, Cu, and O co-exist in different areas and that the intensities of corresponding peaks for different areas show no obvious deviation. This implies the even distribution between SiC and Cu phases in the composite powder.

The morphologies of original SiC and the composite particles are shown in Fig. 3. Different from the original SiC particles in Fig. 3(a), the composite particles consist of very fine adherent Cu crystallites on SiC. The Cu crystallites, whose average diameter is $\sim 50 \text{ nm}$, adhere to SiC particle(s) by physical bonding. Even though the physical bonding types between the inert SiC and Cu

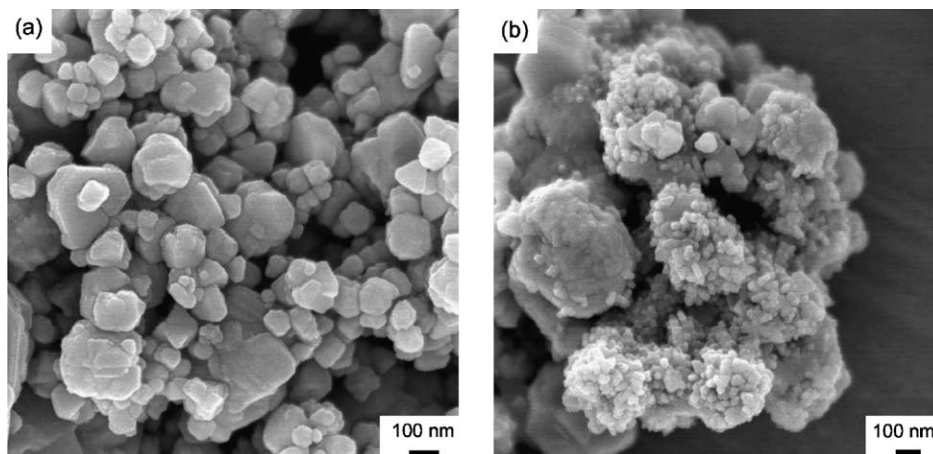


Fig. 3. The morphology of (a): SiC original particles and (b): Cu/SiC composite particles.

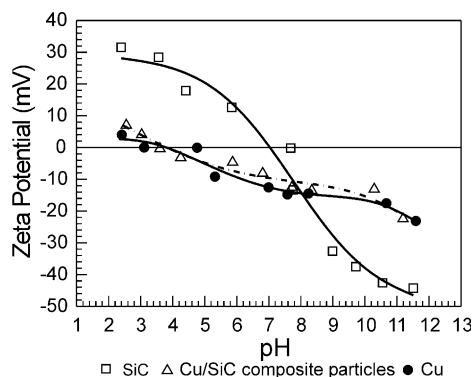


Fig. 4. Changes in zeta potential versus pH of different samples.

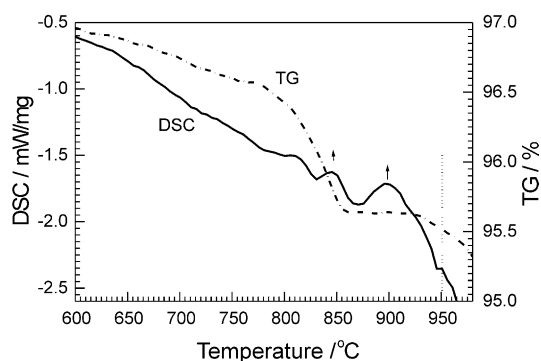


Fig. 5. The DSC-TG curves of the coated Cu/SiC composite particles.

particles are not now fully understood, one of which Van der Waals' attractive forces may function. Meanwhile, the mechanical entrapment might be enhanced through the possible micro surface deformation of the nano Cu crystallites during the coating process. When the settling nano Cu crystallites, which differ structurally and characteristically from the crystalline or glassy state, touch the rotating rigid SiC particle, an instantaneous shear strain might possibly occur at the surface of Cu particle due to the combined effects of relative sliding and the ductility of the nano Cu crystallites [10]. Consecutive steps can be plausibly imagined during the coating process: (1) one Cu crystallite settles and contacts the rotating SiC particle; (2) the Cu crystallite nucleates on the surface and adheres onto the SiC. Once the Cu crystallite is adsorbed, the fluid flow in the vicinity of the rotating SiC particle will be disturbed and an instantaneous negative pressure will be locally generated back to this raised adsorbed Cu crystallite. More Cu crystallites will be sucked and kink to each other successively and incorporate along the SiC particle [13]. Therefore, a core-shell structure is constructed in the coated composite particles with the core of SiC particle(s) and the coating shell of nano Cu crystallites.

From the changes in Zeta potential of different particles shown in Fig. 4, the isoelectric point of the coated

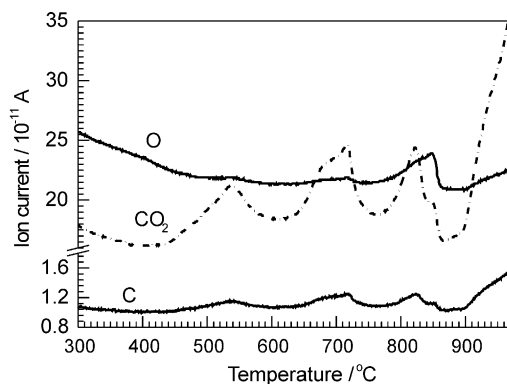


Fig. 6. The MS curves of the coated Cu/SiC composite particles.

composite particles appears at pH 3.6, shifting from pH 7.4 for SiC to pH 3.5 for Cu_2O . Meanwhile, the Zeta potential value is more close to that of Cu_2O rather than that of SiC. This demonstrates that a new surface of Cu_2O is created on the coated Cu/SiC composite particles. The Cu_2O content could be estimated according to the solubility of air in the aqueous solution at the given temperature. The average diameter of the resultant coated composite particles is ~ 270 nm.

Fig. 5 shows the DSC-TG-MS profiles during the heating process. Two obvious endothermic peaks appear at 850 and 900 °C, respectively. Oxygen is detected to release at 850 °C, as shown in Fig. 6, which arises from the decomposition of CuO. Although no CuO (or less than 5 wt.%; within the resolution limit of XRD) is detected in the starting coated particles, it can be formed through the oxidation of Cu_2O (and/or copper) with the entrapped oxygen during the heating process. The decomposition of CuO at 850 °C leads to a weight loss of about 1.0%. The latter endothermic peak implies the melting of Cu_2O /copper eutectic at 900 °C since no corresponding weight loss occurs [14]. It is noticed that, due to the abnormal specific surface area of the nano particles, the temperature at which CuO decomposes or Cu_2O /copper melts is much lower than that reported in the phase diagrams [15,16]. From the changing trend of the DSC curve, a large exothermic peak is supposed at above 950 °C. Correspondingly, the MS curve in Fig. 6 reveals that substantial carbon and CO_2 are formed. This indicates that silicon enters into the solution of liquid copper beyond 950 °C and reacts with copper. As a result, graphite is created [4,17,18]. Therefore, for the Cu/SiC composite particles, the reactions in the system $\text{SiC-Cu-Cu}_2\text{O-C}$ may occur during the heating process. It should be mentioned that the reaction of SiC with copper is very detrimental to the composite as it brings about a decrease of the mechanical properties and should be prevented [19]. Therefore, the desired sintering temperature for the coated Cu/SiC composite particles is lower than 950 °C.

4. Conclusion

A core-shell structure is constructed in the coated nanoscale Cu/SiC composite particles with the core of SiC and the shell of Cu. A new layer of Cu₂O is created on the surface of the coated particles due to the oxidation of nano Cu crystallites. The expected sintering temperature is below 950 °C.

References

- [1] F.E. Kennedy, A.C. Balbahadur, D.S. Lashmore, The friction and wear of Cu-based silicon carbide particulate metal matrix composites for brake applications, *Wear* 203–204 (1997) 715–721.
- [2] J.R. Groza, J.C. Gibeling, Principles of particle selection for dispersion-strengthened copper, *Mater. Sci. Eng. A* 171 (1993) 115–125.
- [3] R.R. Tummala, Ceramic and glass-creamic packaging in the 1990s, *J. Am. Ceram. Soc.* 74 (5) (1991) 895–908.
- [4] F. Delannay, L. Froyen, A. Deruyttere, Review, The wetting of solids by molten metals and its relation to the preparation of metal-matrix composites, *J. Mater. Sci.* 22 (1987) 1–6.
- [5] J. Pelleg, M. Ruhr, M. Ganor, Control of the reaction at the fibre-matrix interface in a Cu/SiC metal matrix composite by modifying the matrix with 2.5 wt.% Fe, *Mater. Sci. Eng. A* 212 (1996) 139–148.
- [6] S.Y. Chang, S.J. Lin, Fabrication of SiCw reinforced copper matrix composite by electroless copper plating, *Scripta Mater.* 35 (2) (1996) 225–231.
- [7] P. Yih, D.D.L. Chung, A comparative study of the coated filler method and the admixture method of powder metallurgy for making metal-matrix composites, *J. Mater. Sci.* 32 (11) (1997) 2873–2882.
- [8] P. Yih, D.D.L. Chung, Silicon carbide whisker copper-matrix composites fabricated by hot pressing copper coated whiskers, *J. Mater. Sci.* 31 (1996) 399–406.
- [9] Y.F. Lee, S.L. Lee, C.L. Chuang, J.C. Lin, Effect of SiCp reinforcement by electroless copper plating on properties of Cu/SiC composites, *Powder Metall.* 42 (2) (1999) 147–152.
- [10] H. Gleiter, Materials with ultrafine microstructures: retrospectives and perspectives, *Nanostructured Mater.* 1 (1992) 1–19.
- [11] R.C. Cammarata, Mechanical properties of nanocomposite thin films, *Thin Solid Films* 240 (1994) 82–87.
- [12] M.B. Bever (Ed.), *Encyclopedia of Materials Science and Engineering*, Pergamon Press, Massachusetts Institute of Technology, USA, Cambridge, Massachusetts, 1986.
- [13] C. Buelens, J.P. Celis, J.R. Roos, Electrochemical aspects of the codeposition of gold and copper with inert particles, *J. Appl. Electrochem.* 13 (1983) 541–548.
- [14] D.E. Jech, J.L. Sepulveda, A.B. Traversone, US patent, US005686676A, 11 November 1997.
- [15] M.K. Reser (Ed.), *Phase Diagrams for Ceramists*, The American Ceramic Society, Columbus, OH, 1969.
- [16] M.K. Reser (Ed.), *Phase Diagrams for Ceramists*, 3rd Edition, The American Ceramic Society, Columbus, OH, 1974.
- [17] Z. An, A. Ohi, M. Hirai, M. Kusaka, M. Iwami, Study of the reaction at Cu/3C-SiC interface, *Surf. Sci.* 493 (2001) 182–187.
- [18] J.S. Park, K. Landry, J.H. Perepezko, Kinetic control of silicon carbide/metal reactions, *Mater. Sci. Eng. A* 259 (1999) 279–286.
- [19] R. Warren, C.-H. Andersson, Silicon carbide fibres and their potential for use in composite materials, Part II, *Composites* 15 (2) (1984) 101–111.